Report

Current Biology

Sensory Feedback Reduces Individuality by Increasing Variability within Subjects

Graphical Abstract

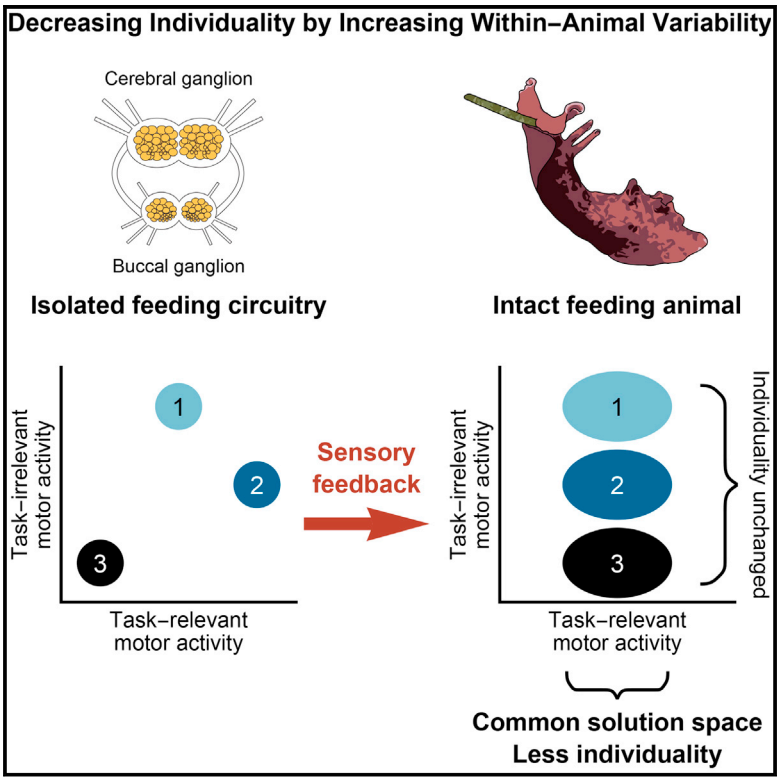

Authors

Miranda J. Cullins, Jeffrey P. Gill, Jeffrey M. McManus, Hui Lu, Kendrick M. Shaw, Hillel J. Chiel

Correspondence

hjc@case.edu

In Brief

Variability is ubiquitous but is not just noise; rather, it may enhance motor behavior. Cullins et al. show that motor patterns for feeding in the marine mollusk *Aplysia* are less individualized when sensory feedback is present. By increasing each animal's pattern variability, sensory feedback provides all animals access to a common solution space.

Highlights

- Without sensory feedback, isolated ganglia motor patterns are very individualized
- Sensory feedback reduces individuality by increasing within-animal motor variability
- High behavioral impact motor components show the largest reductions in individuality
- Sensory feedback effects depend on task, biomechanics, and the environmental context

Cullins et al., 2015, Current Biology *25*, 2672–2676
October 19, 2015
http://dx.doi.org/10.1016/j.cub.2015.08.044

CellPress

Current Biology
Report

Sensory Feedback Reduces Individuality by Increasing Variability within Subjects

Miranda J. Cullins,[1] Jeffrey P. Gill,[1] Jeffrey M. McManus,[1] Hui Lu,[1] Kendrick M. Shaw,[1] and Hillel J. Chiel[1,2,3,*]
[1]Department of Biology, Case Western Reserve University, Cleveland, OH 44106-7080, USA
[2]Department of Neurosciences, Case Western Reserve University, Cleveland, OH 44106-7080, USA
[3]Department of Biomedical Engineering, Case Western Reserve University, Cleveland, OH 44106-7080, USA
*Correspondence: hjc@case.edu
http://dx.doi.org/10.1016/j.cub.2015.08.044

SUMMARY

Behavioral variability is ubiquitous [1–6], yet variability is more than just noise. Indeed, humans exploit their individual motor variability to improve tracing and reaching tasks [7]. What controls motor variability? Increasing the variability of sensory input, or applying force perturbations during a task, increases task variability [8, 9]. Sensory feedback may also increase task-irrelevant variability [9, 10]. In contrast, sensory feedback during locust flight or to multiple cortical areas just prior to task performance decreases variability during task-relevant motor behavior [11, 12]. Thus, how sensory feedback affects both task-relevant and task-irrelevant motor outputs must be understood. Furthermore, since motor control is studied in populations, the effects of sensory feedback on variability must also be understood within and across subjects. For example, during locomotion, each step may vary within and across individuals, even when behavior is normalized by step cycle duration [13]. Our previous work demonstrated that motor components that matter for effective behavior show less individuality [14]. Is sensory feedback the mechanism for reducing individuality? We analyzed durations and relative timings of motor pools within swallowing motor patterns in the presence and absence of sensory feedback and related these motor program components to behavior. Here, at the level of identified motor neurons, we show that sensory feedback to motor program components highly correlated with behavioral efficacy reduces variability across subjects but—surprisingly—increases variability within subjects. By controlling intrinsic, individual differences in motor neuronal activity, sensory feedback provides each subject access to a common solution space.

RESULTS AND DISCUSSION

How might sensory feedback shape motor output? Two sources of variability in a population—within-animal variability and across-animal variability—may be differentially regulated to change overall variability, generating four major alternatives (Figure 1). Animals may converge on a single solution (Figure 1, lower-left quadrant) due to reductions in variability both within and across animals. Second, animals may gain access to a common solution space (Figure 1, lower-right quadrant) by reducing variability across animals but increasing variability within animals. Third, each animal may gain access to a unique solution (Figure 1, upper-left quadrant) by reducing variability within animals, but increasing variability across animals. Finally, animals may gain access to a unique solution space (Figure 1, upper-right quadrant) by increasing variability both within and across animals. The other schematics show changes in only across-animal variability (Figure 1, upper- and lower-middle schematics) or within-animal variability (Figure 1, middle left and right schematics). What are the actual effects of sensory feedback on variability?

To determine how sensory feedback shapes a single motor output, we focused on the power stroke of swallowing in the marine mollusk *Aplysia californica*: the activity of the motor neurons (B8a/B8b; [15]) that keep the grasper closed as it draws seaweed into the buccal cavity during swallowing. We measured the duration of grasper motor neuron activation, normalized by swallow duration. For seven intact, behaving animals, box-and-whisker plots of the normalized durations of motor neuronal activity showed similar median values across animals and similar amounts of variability within each animal (i.e., similar box sizes; Figure 2A). In contrast, when all sensory feedback was removed, and motor programs were induced in seven different pairs of ganglia containing the neural circuitry for feeding behavior (the cerebral and buccal ganglia [17]; the long-lasting cholinergic agonist carbachol was applied to the cerebral ganglion to induce feeding motor programs [16]), box-and-whisker plots of the normalized durations showed greater variation across animals (i.e., very different median values) and great differences in the variability within each animal (Figure 2B). Surprisingly, many of the within-animal variations were smaller than those observed in vivo (compare animals 8, 9, 10, and 14 in Figure 2B with animals 1–6 in Figure 2A). Although a few animals showed large variability in vitro (e.g., animals 11 and 13), black box-and-whisker plots of the pooled durations show that overall variability is lower in vivo than in vitro.

How can within-animal and across-animal variability be quantified? We measured variability within each animal using the interquartile range (IQR; difference in third and first quartiles). We summarized within-animal variability for a group of animals using the median value of the IQRs (see Figure S1). In Figures 2A and 2B, the medians of the IQRs are 18.1% (feedback present) and

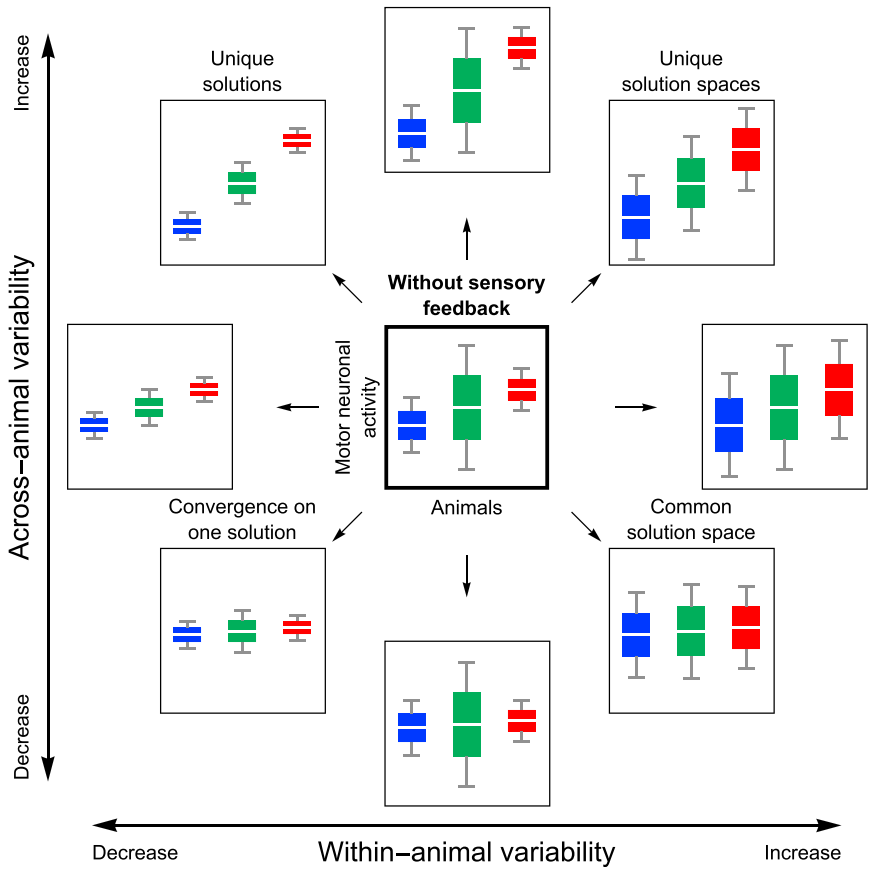

Figure 1. How Sensory Feedback Could Affect Motor Variability

Center square shows a schematic of variability across and within animals in the absence of sensory feedback. Surrounding squares show possible effects of sensory feedback. Within-animal variability may decrease (left) or increase (right) for most animals; similarly, across-animal variability may decrease (bottom) or increase (top) for most animals. Within each square, box-and-whisker plots for data from three subjects are shown. Bottom and top whiskers correspond to the smallest and largest values, respectively; bottom and top of box correspond to the first and third quartile, respectively; the line within each box is the median value.

9.2% (feedback absent), so the net change in within-animal variability is 18.1% − 9.2% = 8.9% (i.e., within-animal variability increases when sensory feedback is present). We summarized across-animal variability using the IQR of the medians of all animals in the group (see Figure S1). In Figures 2A and 2B, the IQRs of the medians are 3.8% (feedback present) and 17.6% (feedback absent), respectively, so the net change in across-animal variability is 3.8% − 17.6% = −13.8% (i.e., across-animal variability decreases when sensory feedback is present). Thus, the change in within-animal and across-animal variability is (+8.9%, −13.8%); this point, representing the data in Figure 2, is highlighted by a small square in Figure 3A.

Although these measures quantify changes in components of variability, they do not quantify how different animals are from each other, i.e., the individuality within a group of animals. A statistic can be derived from the Mann-Whitney test that summarizes variability within and across animals, defining individuality. By comparing ranks to determine whether one animal tends to produce longer normalized motor neuronal durations than a second animal, the Mann-Whitney test can distinguish two animals from one another; the test generates a U statistic. The effect size, that is, how different (how individual) two animals are from one another, can then be obtained by normalizing the U statistic by the product of the number of responses in each animal. The normalized U statistic is mathematically equivalent to computing the area under the curve (AUC) of a receiver operating characteristic (ROC) curve [18]. To determine the overall individuality, one averages normalized U statistics from each pairwise comparison of the animals [19]. The resulting statistic will be referred to as the average AUC. It ranges from 0.5, indicating that animals cannot be distinguished from one another, to 1.0, indicating that animals are completely distinct from one another (Figures S2A1–S2B2). In general, high within-animal variability will make animals harder to distinguish as individuals even if there is across-animal variability and will lower the average AUC.

Normalized durations in vivo are significantly less individual than those recorded in the isolated ganglia (average AUC in vivo = 0.610, Figure 2A; average AUC in isolated ganglia = 0.731, Figure 2B; $p < 0.00002$, bootstrapping, two-tailed test). The results are consistent with the hypothesis that sensory feedback reduces individuality by decreasing variability across animals, but—unexpectedly—sensory feedback increases variability within animals, so that all animals gain access to a common solution space (Figure 1, lower-right quadrant).

To control for the possibility that pharmacological effects of carbachol were responsible for the greater individuality observed in isolated ganglia motor patterns, we analyzed motor patterns in a preparation in which carbachol induced motor patterns but sensory feedback was intact: the suspended buccal mass (SBM) [20]. The SBM performs swallowing movements when fed seaweed strips identical to those used in vivo. Individuality in normalized durations of motor neuronal activity was not significantly different from in vivo but was significantly different from the isolated ganglia (average AUC in the SBM = 0.670; not significantly different from in vivo, $p = 0.13$, bootstrapping, two-tailed test; significantly less individual than the isolated ganglia, $p = 0.019$, bootstrapping, two-tailed test; see Figure S2C). Thus, motor patterns induced in vitro using carbachol in the presence of sensory feedback are not statistically different in individuality from those observed in vivo, so the changes observed in the isolated ganglia are not due to the pharmacological effects of carbachol but to the absence of sensory feedback.

How does sensory feedback affect all motor program components for swallowing? We measured the activities of most identified motor neurons recruited during swallowing in *Aplysia*. From

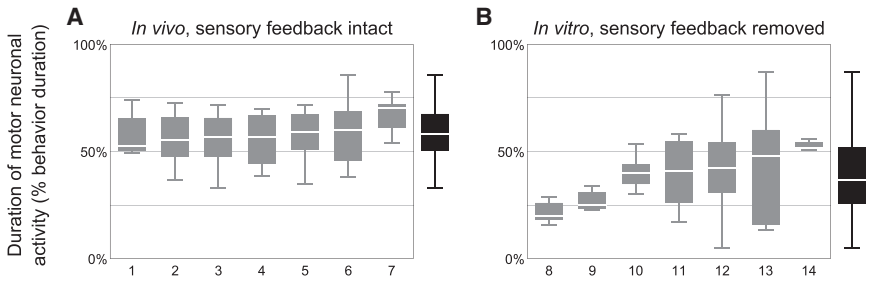

Figure 2. Effect of Sensory Feedback on a Behaviorally Relevant Motor Neuron

On average, variability across animals decreases but within animals increases in the presence of sensory feedback for a behaviorally relevant motor neuron.

(A) Box-and-whisker plots for the normalized duration of grasper motor neuron (B8a/B8b) activity recorded in seven different intact, behaving animals during multiple swallows induced by seaweed strips (n = 7, 10, 23, 5, 18, 9, and 7 swallows, respectively).

(B) Box-and-whisker plots for the normalized grasper motor neuron duration recorded in seven cerebral and buccal ganglia, in which motor programs were induced by application of the long-lasting cholinergic agonist carbachol to the cerebral ganglion [16] (n = 9, 7, 10, 18, 23, 7, and 5 ingestive motor patterns, respectively). The variability within several isolated ganglia without sensory feedback (animals 8, 9, 10, and 14) is lower than that observed in intact animals. In some isolated ganglia, within-animal variability increases (animals 11 and 13).

The black box-and-whisker plots to the right of (A) and (B) combine the data from animals in each group; the overall variability is clearly lower in vivo than in vitro. Meanings of box components and whiskers are given in the legend for Figure 1.

extracellular recordings, we determined durations and overlaps of motor pool activity for each swallow, normalized by dividing by behavior duration; we refer to these as "motor program components" (a total of 45, corresponding to the points in Figure 3; see Figure S3A and Supplemental Information). If sensory input guides subjects to a precise response, most motor program components should show reduced within-animal variability (Figure 1, left). Rather surprisingly, we found that almost all motor program components showed increases in within-animal variability (Figure 3A, whose axes are analogous to those of Figure 1; note that points fall largely to the right; $p = 2.8 \times 10^{-8}$, Wilcoxon signed-rank two-tailed test). Collectively, the motor program components showed no net change in across-animal variability ($p = 0.24$, Wilcoxon signed-rank two-tailed test).

Does sensory feedback differentially affect motor program components that are more important for effective behavior? To determine each motor neuron's behavioral impact, we quantified the correlations between measures of swallowing efficacy and each motor program component using Spearman's rank correlation coefficient, ρ. Because both inward and outward movement of seaweed must be regulated for successful swallowing, these movements were measured, and the higher correlation of either movement with a motor program component was chosen (the significance of each correlation was not tested and therefore did not need to be corrected for multiple comparisons). Correlations of motor program components with net inward movement (inward minus outward movement) yielded similar results. When the motor program components are sorted by behavioral impact, measures strongly correlated with behavioral efficacy ($|\rho| \geq 0.3$) showed a significant decrease in across-animal variability in the presence of sensory feedback (Figure 3A; note that the bright green points are mostly below the central horizontal axis; $p = 0.013$, Wilcoxon signed-rank two-tailed test). In contrast, measures weakly correlated with behavioral efficacy ($|\rho| < 0.3$) showed a significant increase in across-animal variability (Figure 3A; note that the dark points are mostly above the central horizontal axis; $p = 0.0007$, Wilcoxon signed-rank two-tailed test). Thus, motor program components with high behavioral impact showed both an increase in within-animal variability and a decrease in across-animal variability, suggesting that these motor components were brought into a common solution space (Figures 1 and 3A, lower-right quadrants). The results shown for a single motor program component (Figure 2) are therefore typical of how sensory feedback shapes variability in motor program components that have high behavioral impact.

Analysis of all motor program components demonstrated that changes in within- and across-animal variability due to sensory feedback were correlated (Figure 3A; Spearman's $\rho = 0.600$, $p = 0.00001$). This correlation suggested that use of the individuality statistic (average AUC) to capture both aspects of variability would provide greater insight into the role of sensory feedback.

Sensory feedback acts to reduce individuality in those motor program components with high behavioral impact. Figure 3B plots, for each motor program component, the change in individuality resulting from the addition of sensory feedback versus the behavioral impact of that motor program component. For example, the change in individuality for normalized grasper motor neuron duration from in vitro (Figure 2B, AUC = 0.731) to in vivo (Figure 2A, AUC = 0.610) is $0.610 - 0.731 = -0.121$. The behavioral impact for this measure was $|\rho| = 0.39$. The resulting point, $(-0.121, 0.39)$, is highlighted in Figure 3B by a small square. Motor program components that have moderate to large behavioral impact ($|\rho| \geq 0.3$) always show decreases in individuality when sensory feedback is present (Figure 3B; Spearman's $\rho = -0.588$, $p = 0.00002$). Similar results were obtained when motor program components in the control (SBM) were compared with the isolated ganglia (Figure S3B), suggesting that these effects are attributable to sensory feedback rather than the use of carbachol to induce patterns in vitro. Furthermore, comparisons of changes in individuality and behavioral impact from the motor program components in the control to in vivo were not significant (Spearman's $\rho = 0.263$, $p = 0.08$). These results demonstrate that sensory feedback reduces differences among subjects in motor program components that have high behavioral impact and that it does so by increasing within-animal variability and decreasing across-animal variability.

Rather surprisingly, this study demonstrates that sensory feedback can act to increase one form of variability (within-animal variability) to minimize differences intrinsic to each nervous system, thus giving all animals access to a common solution space, and that this form of sensory shaping is primarily

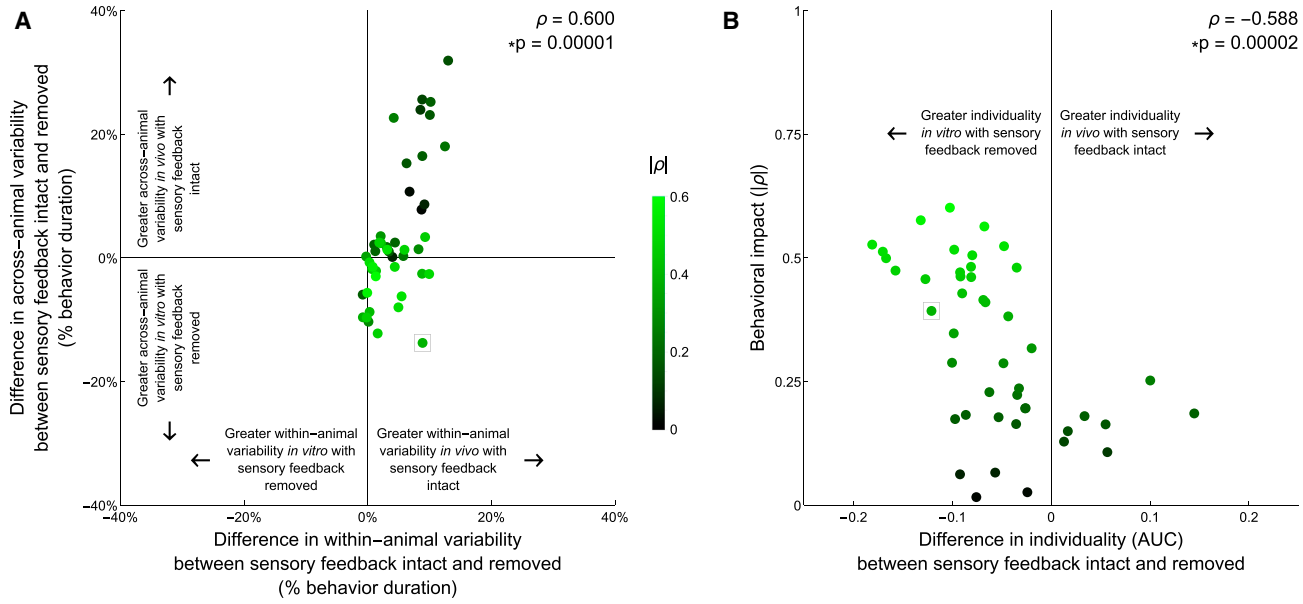

Figure 3. Sensory Feedback Selectively Decreases Individuality

In the presence of sensory feedback, behavioral impact is associated with decreased across-animal variability and increased within-animal variability and thus decreased individuality.

(A) Sensory feedback in vivo can induce decreases in across-animal variability and increases in within-animal variability. Plot axes are analogous to those of Figure 1. Each point represents the change in within-animal and across-animal variability in a single motor program component (Figure S3A). The change in variability of the data in Figure 2 is highlighted by a small square in Figure 3A (see text for details). Each motor program component was evaluated for its behavioral impact (see text). Points are colored from black (low behavioral impact) to green (high behavioral impact; scale between panels A and B). Changes in within- and across-animal variability are strongly correlated.

(B) Components with high behavioral impact always show decreases in individuality (average AUC) when sensory feedback is present. In contrast, motor program components with low behavioral impact show both increases and decreases in individuality when sensory feedback is present. Data from Figure 2 are highlighted by a small square in Figure 3B (see text for details).

addressed to those motor program components with greatest behavioral impact. Among other causes, within-animal variability may be due to changes in sensory input, the animal's internal state (e.g., food arousal), and the actual effectiveness of its behavior in consuming seaweed. Thus, the study demonstrates the importance of determining how sensory feedback affects both within-animal and across-animal variability rather than simply measuring the variability of a population. It also strongly supports prior work that demonstrates that one must determine the biomechanical context and the task relevance of motor program components to understand how sensory feedback is addressed to each one [10, 21, 22].

The framework we have presented (Figure 1) is of general interest because sensory feedback may shape motor variability in different ways depending on biomechanical, task, and environmental constraints. If a motor behavior has only one "correct" solution, sensory feedback may enforce convergence on a single solution (Figure 1, lower-left quadrant) [23]. If subjects can specialize successfully using different very precise solutions, then sensory feedback may help them generate unique solutions (Figure 1, upper-left quadrant) [24]. Increases in variability both within and across animals may also be important (Figure 1, upper-right quadrant); indeed, increases in both kinds of variability were found in many of the motor program components that had the lowest correlation with behavioral efficacy (Figure 3A). How could increasing variability in these motor program components be useful? Reduction of variability for motor program components strongly related to behavioral expression may take advantage of increases in variability of components of the motor system that are not task related [9]. Furthermore, the sum of two or more components may be tightly regulated, even if the individual components show considerable apparent variability [10]. More generally, multiple combinations of degrees of freedom that can generate essentially identical outputs (the "uncontrolled manifold" [25]) may show high variability in components but show low variability after the components are appropriately combined based on an animal's neural or biomechanical structure [25, 26].

That animals may need to work within a common solution space is consistent with a recent shift in thinking about motor systems. For some time, it was assumed that motor systems compute globally optimal solutions to obtain highly precise trajectories to targets [27]. A radical shift has occurred in thinking about motor systems. Studies of motor control have begun to focus on the vital importance of variability for solving motor problems. Having a myriad of readily accessible "good enough" solutions may be preferable to computing a global optimum, especially in complex, changing environments [27–30].

These studies can clarify the cellular and synaptic mechanisms by which sensory feedback shapes motor variability. For example, after determining that deafferentation increased elevator phase variability in locust flight, Wolf and Pearson were able to find the key synaptic input to crucial elevator

interneurons [31, 32]. More generally, focusing on the specific motor program components whose variability is shaped by sensory feedback and how that variability is shaped can guide cellular studies in many other systems.

SUPPLEMENTAL INFORMATION

Supplemental Information includes Supplemental Experimental Procedures and three figures and can be found with this article online at http://dx.doi.org/10.1016/j.cub.2015.08.044.

AUTHOR CONTRIBUTIONS

M.J.C. designed and did in vivo experiments, analyzed data, created figures, and contributed to writing the paper. J.P.G. did the statistical analysis of the data, created figures, and contributed to writing the paper. J.M.M. and H.L. did the in vitro experiments. K.M.S. helped with the statistical analysis of the data. H.J.C. helped design the experiments and analyze the data and wrote the paper.

ACKNOWLEDGMENTS

This work was supported by NIH NS-047073, NSF DMS-1010434, and IIS-1065489. We thank Emilie Lothet, Dr. Roberto Galán, and two anonymous reviewers for helpful comments.

Received: April 30, 2015
Revised: July 17, 2015
Accepted: August 19, 2015
Published: October 1, 2015

REFERENCES

1. Graham, D. (1985). Pattern and control of walking in insects. Adv. In Insect Phys. *18*, 31–140.
2. Winter, D.A., and Yack, H.J. (1987). EMG profiles during normal human walking: stride-to-stride and inter-subject variability. Electroencephalogr. Clin. Neurophysiol. *67*, 402–411.
3. Heinzel, H.-G. (1988). Gastric mill activity in the lobster. I. Spontaneous modes of chewing. J. Neurophysiol. *59*, 528–550.
4. Herzog, W., Zatsiorsky, V., Prilutsky, B.I., and Leonard, T.R. (1994). Variations in force-time histories of cat gastrocnemius, soleus and plantaris muscles for consecutive walking steps. J. Exp. Biol. *191*, 19–36.
5. Davids, K., Bennett, S., and Newell, K., eds. (2006). Movement System Variability (Champaign: Human Kinetics).
6. Cappellini, G., Ivanenko, Y.P., Poppele, R.E., and Lacquaniti, F. (2006). Motor patterns in human walking and running. J. Neurophysiol. *95*, 3426–3437.
7. Wu, H.G., Miyamoto, Y.R., Gonzalez Castro, L.N., Ölveczky, B.P., and Smith, M.A. (2014). Temporal structure of motor variability is dynamically regulated and predicts motor learning ability. Nat. Neurosci. *17*, 312–321.
8. Trommershäuser, J., Gepshtein, S., Maloney, L.T., Landy, M.S., and Banks, M.S. (2005). Optimal compensation for changes in task-relevant movement variability. J. Neurosci. *25*, 7169–7178.
9. Diedrichsen, J., Shadmehr, R., and Ivry, R.B. (2010). The coordination of movement: optimal feedback control and beyond. Trends Cogn. Sci. *14*, 31–39.
10. Todorov, E. (2004). Optimality principles in sensorimotor control. Nat. Neurosci. *7*, 907–915.
11. Pearson, K.G., and Wolf, H. (1987). Comparison of motor patterns in the intact and deafferented flight system of the locust. I. Electromyographic analysis. J. Comp. Physiol. A *160*, 259–268.
12. Churchland, M.M., Yu, B.M., Cunningham, J.P., Sugrue, L.P., Cohen, M.R., Corrado, G.S., Newsome, W.T., Clark, A.M., Hosseini, P., Scott, B.B., et al. (2010). Stimulus onset quenches neural variability: a widespread cortical phenomenon. Nat. Neurosci. *13*, 369–378.
13. Dingwell, J.B., Cusumano, J.P., Cavanagh, P.R., and Sternad, D. (2001). Local dynamic stability versus kinematic variability of continuous overground and treadmill walking. J. Biomech. Eng. *123*, 27–32.
14. Cullins, M.J., Shaw, K.M., Gill, J.P., and Chiel, H.J. (2015). Motor neuronal activity varies least among individuals when it matters most for behavior. J. Neurophysiol. *113*, 981–1000.
15. Morton, D.W., and Chiel, H.J. (1993). The timing of activity in motor neurons that produce radula movements distinguishes ingestion-like and rejection-like motor patterns in a reduced preparation of *Aplysia*. J. Comp. Physiol. A *173*, 519–536.
16. Susswein, A.J., Rosen, S.C., Gapon, S., and Kupfermann, I. (1996). Characterization of buccal motor programs elicited by a cholinergic agonist applied to the cerebral ganglion of *Aplysia californica*. J. Comp. Physiol. A Neuroethol. Sens. Neural Behav. Physiol. *179*, 509–524.
17. Kupfermann, I. (1974). Dissociation of the appetitive and consummatory phases of feeding behavior in *Aplysia*: a lesion study. Behav. Biol. *10*, 89–97.
18. Acion, L., Peterson, J.J., Temple, S., and Arndt, S. (2006). Probabilistic index: an intuitive non-parametric approach to measuring the size of treatment effects. Stat. Med. *25*, 591–602.
19. Hand, D.J., and Till, R.J. (2001). A simple generalisation of the area under the ROC curve for multiple class classification problems. Mach. Learn. *45*, 171–186.
20. McManus, J.M., Lu, H., and Chiel, H.J. (2012). An *in vitro* preparation for eliciting and recording feeding motor programs with physiological movements in *Aplysia californica*. J. Vis. Exp. *70*, e4320, http://dx.doi.org/10.3791/4320.
21. Hultborn, H. (2001). State-dependent modulation of sensory feedback. J. Physiol. *533*, 5–13.
22. Knill, D.C., Bondada, A., and Chhabra, M. (2011). Flexible, task-dependent use of sensory feedback to control hand movements. J. Neurosci. *31*, 1219–1237.
23. Zhang, W., Scholz, J.P., Zatsiorsky, V.M., and Latash, M.L. (2008). What do synergies do? Effects of secondary constraints on multidigit synergies in accurate force-production tasks. J. Neurophysiol. *99*, 500–513.
24. Handford, C. (2006). Serving up variability and stability. In Movement System Variability, K. Davids, S. Bennet, and K. Newell, eds. (Champaign: Human Kinetics), pp. 73–84.
25. Scholz, J.P., and Schöner, G. (1999). The uncontrolled manifold concept: identifying control variables for a functional task. Exp. Brain Res. *126*, 289–306.
26. Beer, R.D., Chiel, H.J., and Gallagher, J.C. (1999). Evolution and analysis of model CPGs for walking: II. General principles and individual variability. J. Comput. Neurosci. *7*, 119–147.
27. Loeb, G.E. (2012). Optimal isn't good enough. Biol. Cybern. *106*, 757–765.
28. Horn, C.C., Zhurov, Y., Orekhova, I.V., Proekt, A., Kupfermann, I., Weiss, K.R., and Brezina, V. (2004). Cycle-to-cycle variability of neuromuscular activity in *Aplysia* feeding behavior. J. Neurophysiol. *92*, 157–180.
29. Hooper, S.L. (2004). Variation is the spice of life. Focus on "Cycle-to-cycle variability of neuromuscular activity in Aplysia feeding behavior". J. Neurophysiol. *92*, 40–41.
30. Ting, L.H., Chiel, H.J., Trumbower, R.D., Allen, J.L., McKay, J.L., Hackney, M.E., and Kesar, T.M. (2015). Neuromechanical principles underlying movement modularity and their implications for rehabilitation. Neuron *86*, 38–54.
31. Wolf, H., and Pearson, K.G. (1989). Comparison of motor patterns in the intact and deafferented flight system of the locust. III. Patterns of interneuronal activity. J. Comp. Physiol. A *165*, 61–74.
32. Wolf, H. (1993). The locust tegula: significance for flight rhythm generation, wing movement control and aerodynamic force production. J. Exp. Biol. *182*, 229–253.

Current Biology

Supplemental Information

Sensory Feedback Reduces Individuality by Increasing Variability within Subjects

Miranda J. Cullins, Jeffrey P. Gill, Jeffrey M. McManus, Hui Lu, Kendrick M. Shaw, and Hillel J. Chiel

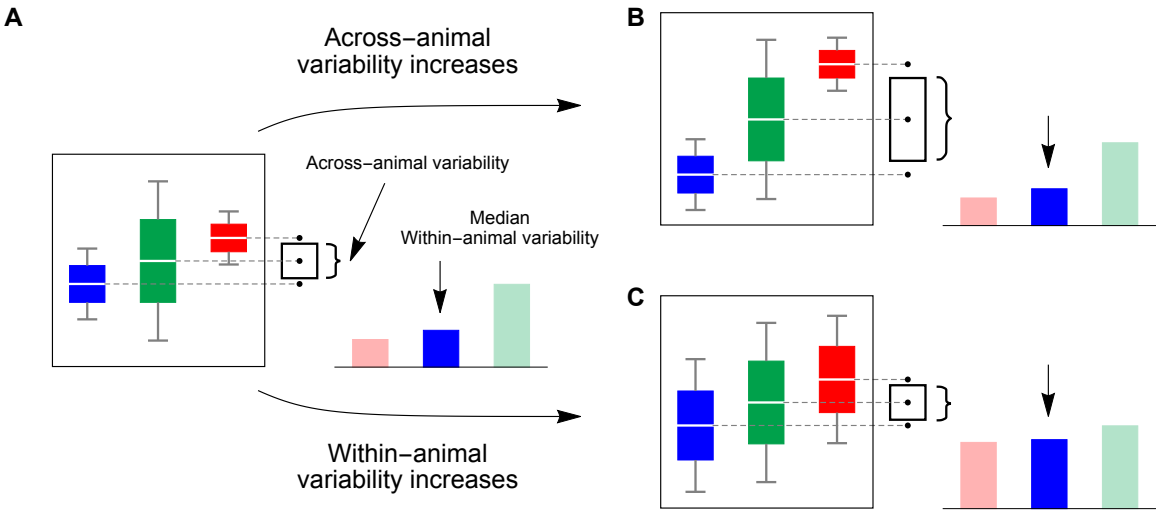

Figure S1 (Related to Figure 1 and the main text) Calculating changes in within-animal and across-animal variability. A. The central box from Figure 1 is shown. To determine the *within-animal* variability, the interquartile ranges are calculated (shown as a bar chart to the right of the original data), and the median of the interquartile ranges is determined (arrow pointing to blue bar, labeled "Within-animal variability"). To determine the *across-animal* variability, the medians are calculated (dashed lines join the median values to the corresponding points to the immediate right of the box-and-whisker plots). The curly bracket shows the interquartile range of the medians (white box; pointed to by arrow labeled "Across-animal variability"). B. Effect of increasing the across-animal variability alone (top box in Figure 1). The medians have separated, so that the white box marked with the curly bracket is larger than that in A. However, the median of the interquartile ranges (arrow pointing to the blue bar) is unchanged. C. Effect of increasing the within-animal variability without affecting the across-animal variability (right box in Figure 1). The within-animal variability has increased, so the median value for the interquartile ranges has increased (arrow pointing to blue bar). The medians have not changed, so the white box marked with the curly bracket is the same size as the box in A.

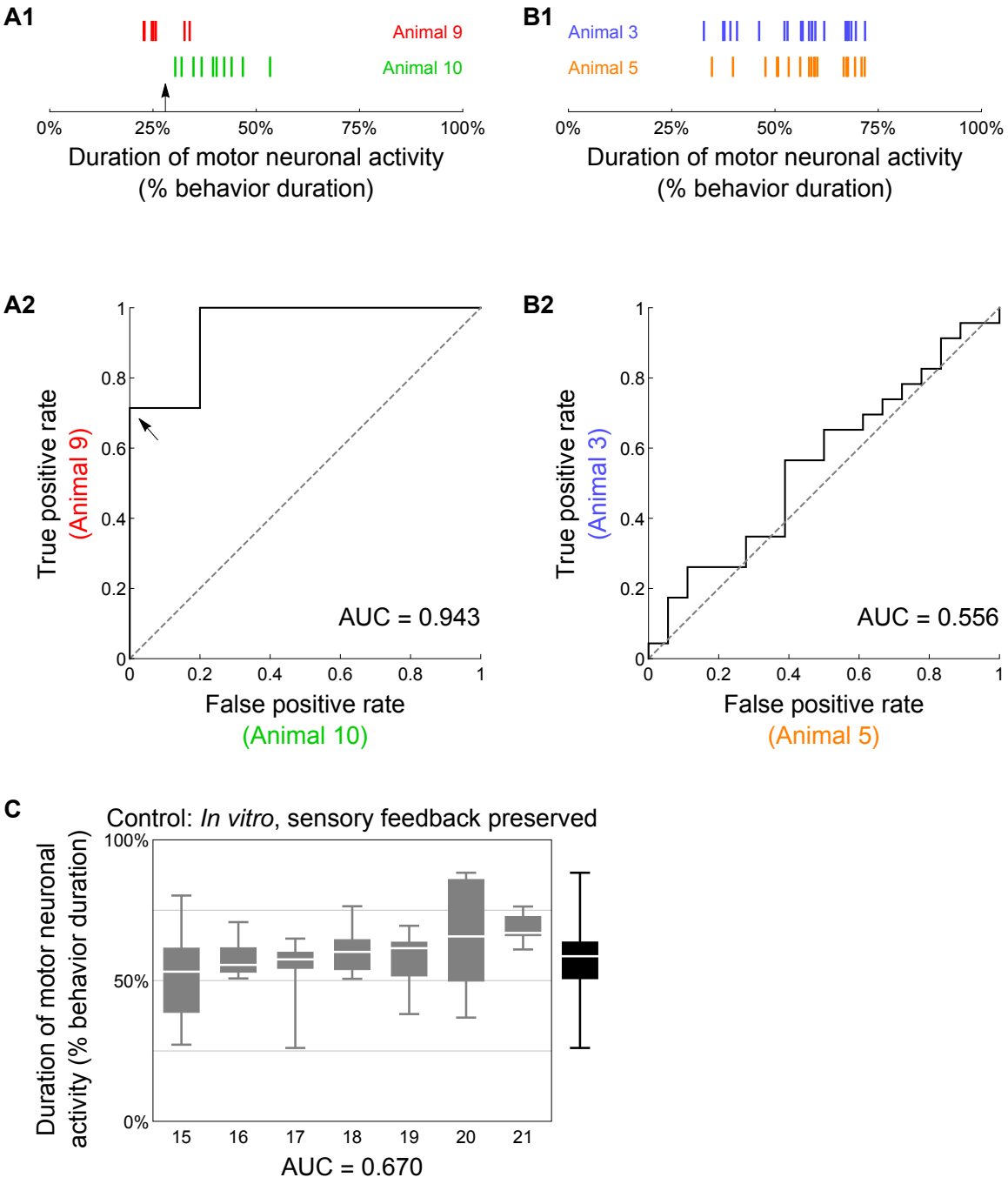

Figure S2. (Related to Figure 2 and Supplemental Experimental Procedures) Computation of the area under the curve (AUC) of a receiver operating characteristic (ROC) curve, and control experiment for comparing variability of *in vivo* and *in vitro* motor patterns. A1. A one-dimensional (1-D) scatter plot of the normalized motor neuronal durations for animals 9 and 10 in Figure 2B. A2. If one attempts to classify normalized durations that are below some threshold as coming from animal 9 and above the threshold as coming from animal 10, a parametric plot of the ROC curve shows that some choices of the threshold yield high true positive classification rates (correct classification of normalized durations from animal 9) and low false positive classification

rates (incorrect classification of normalized durations from animal 10). For example, if the location of the arrow in part A1 is used as the threshold, the ROC curve indicates—at the point marked by the arrow in A2—that the true positive classification rate will be roughly 71% (meaning that 71% of animal 9's normalized durations will be correctly classified), and the false positive classification rate will be 0% (meaning that none of animal 10's normalized durations will be incorrectly classified). The normalized durations from these animals are easy to classify in this way because the distributions are very *dissimilar*, i.e., these animals have *high individuality*. The AUC (0.943) is close to its maximum value of 1, indicating that attempts to classify normalized durations from these animals will have a high rate of success. B1. A 1-D scatter plot of the normalized motor neuronal durations for animals 3 and 5 in Figure 2A. B2. In the same classification problem, the true positive classification rate (correct classification of normalized durations from animal 3) and false positive classification rate (incorrect classification of normalized durations from animal 5) will be approximately equal for any choice of the threshold. Since the distributions are very *similar*, these animals have *low individuality*. The AUC (0.556) is close to its minimum value of 0.5, indicating that attempts to classify normalized durations from these animals will fare not much better than chance. C. In the suspended buccal mass, ingestive patterns were induced using the long-lasting cholinergic agonist carbachol, and swallows were induced using seaweed strips, in seven different preparations. Box-and-whisker plots are shown of the normalized grasper motor neuron durations in these preparations. Even though motor patterns are induced by carbachol, in the presence of sensory feedback from the feeding apparatus, individuality among these animals is less than in the absence of sensory feedback (Figure 2B) but not different from *in vivo* (Figure 2A; see main text for details). Meanings of box components and whiskers are given in the legend for Figure 1.

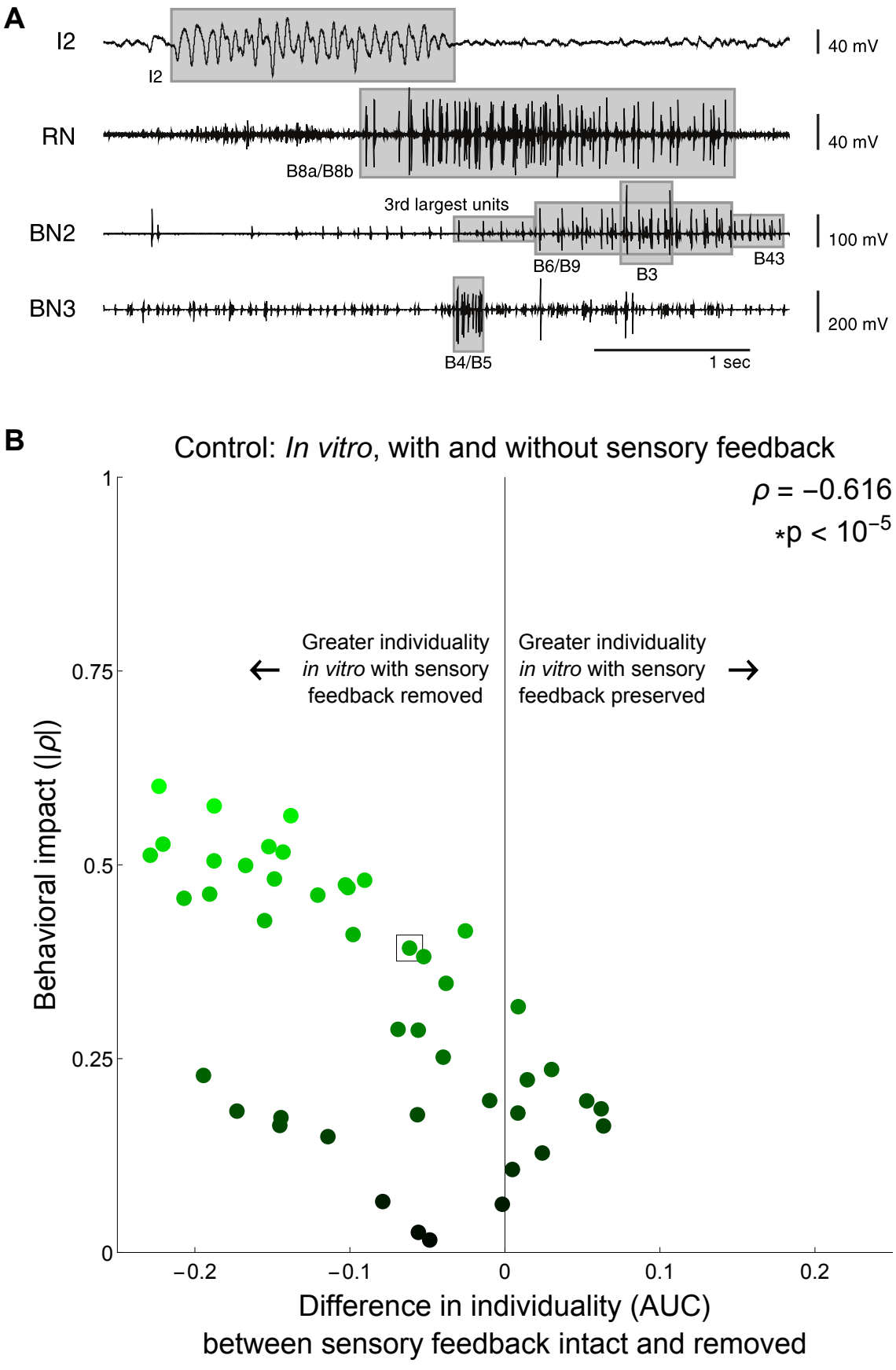
A
I2
I2
40 mV
RN
B8a/B8b
40 mV
3rd largest units
BN2
B6/B9
B3
B43
100 mV
BN3
B4/B5
1 sec
200 mV
B
Control: In vitro, with and without sensory feedback
ρ = −0.616
*p < 10−5
Greater individuality in vitro with sensory feedback removed
Greater individuality in vitro with sensory feedback preserved
Behavioral impact (|ρ|)
1
0.75
0.5
0.25
0
−0.2
−0.1
0
0.1
0.2
Difference in individuality (AUC)
between sensory feedback intact and removed

Figure S3. (Related to Figure 3 and Supplemental Experimental Procedures) Measurements of motor neuronal activity, and control experiment for comparing individuality of *in vivo* and *in vitro* motor patterns. A. The motor pattern for a single *in vivo* swallow simultaneously recorded from three key nerves (buccal nerves 2 and 3 (BN2, BN3) and the radular nerve (RN)) and the protractor muscle I2, indicating the start and stop times of individual motor neuronal units (or of activity due to motor neurons B31/B32, B61/B62 on protractor muscle I2). Identical algorithms were used to detect start and stop times in all three experimental groups. Unit window sizes were unique to each animal. B. Control experiment for comparing individuality in the presence and absence of sensory feedback *in vitro*. Changes in individuality (average AUC) for each motor component in the control (suspended buccal mass, SBM) relative to the isolated ganglion are plotted along the x-axis. Note that for both preparations, motor programs are induced using carbachol, but in the SBM, sensory feedback from the feeding apparatus is present, and swallowing is induced using a seaweed strip. Those motor components most associated with behavioral efficacy (highest behavioral impact, $|\varrho|$) show only decreases in individuality when sensory feedback is present, whereas ones less associated with behavioral efficacy show decreases or increases in individuality when sensory feedback is present.

Supplemental Experimental Procedures

Animals

Aplysia californica weighing 350-450g (Marinus, Long Beach, CA) were kept in aerated tanks (189 liters) of circulating artificial seawater (Instant Ocean, Mentor, OH) at 16˚C in a controlled 12 h/12 h light/dark cycle. Animals were fed seaweed every other day; feeding was stopped 1-2 days before surgery to increase feeding behavior. Animals were selected based on previously described criteria for determining that they were healthy and capable of feeding [S1].

In vivo preparation

To determine relationships among the different motor neuronal units, they must be measured simultaneously. A novel technique [S2] simultaneously implants extracellular electrodes that record from the I2 protractor muscle and all three nerves critical for feeding behavior (buccal nerve 2 (BN2), buccal nerve 3 (BN3), and the radular nerve (RN)). *In vivo* feeding motor patterns (Figure S3A) were recorded from 7 *Aplysia* using this technique. A total of 173 swallows were analyzed.

Electrode signals were recorded using an AC-coupled differential amplifier (model 1700, AM Systems, Everett, WA) using a gain of 10, a low-pass filter set at 1 kHz, and a high-pass filter set to 100Hz for nerve recordings, or set to 10Hz for muscle recordings. Signals were sampled at 2-5 kHz and recorded on a PC using Axoscope (Molecular Devices, Sunnyvale, CA).

Behavior was recorded using a digital videocamera (Canon ZR850, Tokyo, Japan) and synchronized to the neural recordings, using an LED counter (Veeder-Root LED Totalizer, model C342-0562) visible in the video whose update pulse (at 10 Hz) was also recorded in Axoscope [S3]. Seaweed pieces were held against the lips on each side of the mouth to elicit biting and to orient the animal into the camera view. Seaweed strips 0.25 cm wide, marked at 1 cm intervals, evoked swallows. Inward and outward movements of the seaweed strip were measured. The swallows whose recordings and behavior could be analyzed simultaneously were n = 65 swallows from seven animals.

Suspended buccal mass (SBM)

In the *in vitro* suspended buccal mass (SBM) preparation, carbachol-induced feeding movements can be observed with the feeding apparatus and its sensory feedback intact [S4]. The buccal mass was dissected out with the buccal and cerebral ganglia attached. Hook electrodes were applied to the I2 muscle, RN, BN2 and BN3 for motor program measurements, as was done *in vivo* [S2]. The buccal mass and the buccal and cerebral ganglia were placed in a custom-made dish that isolated the cerebral ganglion from the buccal mass and ganglia, so that the cholinergic agonist carbachol (10 mM in *Aplysia* saline) could be applied to the cerebral ganglion alone to elicit ingestive motor programs [S5]. To suspend the buccal mass, a silk suture was threaded through the tissue antero-dorsal to the jaws and attached to the side of the dish. Swallows were obtained by

placing a strip of seaweed (10 cm long, 0.25 cm wide) in the feeding grasper during carbachol-induced bites.

Isolated ganglia

Cerebral and buccal ganglia were dissected out of *Aplysia*, connected via the cerebral-buccal connectives, with a small section of the I2 muscle attached to the I2 nerve. Suction electrodes were applied to the I2 muscle, RN, BN2 and BN3. The ganglia were placed in a dish that isolated the cerebral from the buccal ganglion, and ingestive motor programs were induced by applying carbachol (10 mM) to the cerebral ganglion.

Durations of motor neuronal activity and their correlations with behavioral efficacy

In every animal, for every swallow, we characterized key motor program components, which were the durations and overlaps of activity of motor neurons in the motor pools that were recorded (Figure S3A): start and stop times of I2 during the protraction phase when the muscle EMG rose above 10 Hz and fell below 5 Hz, respectively (related to the activity in the two B31/B32 interneurons and the two B61/B62 motor neurons [S6]; 2 measures), start and stop times of the largest units on RN (corresponding to activity in the two B8a/B8b motor neurons [S3, S7]; 2 measures), start and stop times of the extracellular units from the two B4/B5 neurons on BN3 (largest units on BN3 [S8] from the first to the last spike; 2 measures), and start and stop times of identified motor neurons B6 and B9, and motor neuron B43 [S9] (4 measures). Finally, we measured the third largest units on BN2 [S7, S10, S11], focusing on when they began in retraction (1 measure), for a total of 11 different motor program measures. Although we could identify start and stop times for B3 (largest extracellular unit on BN2 [S9]) when the neuron was active, it was not active in all motor patterns, so we did not include it in further analysis. We have separately analyzed B3's role in biting versus swallowing in a recent publication [S12].

Custom *Mathematica* software identified spikes, calculated and interpolated the instantaneous firing frequencies, created a firing frequency envelope, and determined the start and end times of the main burst for each unit [S13]. After automated measurements were generated, they were verified manually and corrections made by two investigators working independently (as in [S3]).

Absolute timings of single motor measures may not be as useful for characterizing motor patterns as relative timings, durations, and overlaps [S3]. Since we had no *a priori* reason to assume that a particular difference was significant, the pairwise differences of all measured motor features were analyzed. The eleven start and end times described above then generated (11*10)/2 = 55 timing differences. Times were normalized by behavior duration (time from start I2 activity to end B43 activity), yielding 45 normalized motor measures. These correspond to the 45 points shown in Figures 3A and 3B.

Correlation with behavioral efficacy was determined by computing each normalized motor measure's rank correlation coefficient (Spearman's ϱ) with behavioral measures of swallowing efficacy (i.e., inward and outward seaweed movement during a swallow).

Measuring individuality

Receiver operating characteristic (ROC) curves evaluate the effectiveness of a given measure for classifying groups [S14, S15]. The *area under* an ROC *curve* (AUC) measures discriminator efficacy [S14] (Figure S2, parts A1 through B2). To determine how well each motor measure discriminated among the seven experimental animals, the AUC for each pair of animals was computed and averaged to construct a mean AUC for each discriminator [S16] as a measure of overall individuality.

Differences in individuality in normalized duration of RN activity between the isolated ganglia preparation (Figure 2B) and both the *in vivo* and SBM preparations (Figures 2A and S2C) were tested for significance by bootstrapping, as is recommended for averaged AUCs [S16]. Isolated ganglia motor patterns were resampled with replacement for each preparation from among its actual motor patterns, and the average AUC for the normalized duration of RN activity was recalculated. This resampling was performed 50,000 times to generate a distribution. A two-tailed test was then performed to determine if the *in vivo* and SBM average AUCs are significantly different from the isolated ganglia average AUC.

We performed a *post hoc* power analysis by using the same bootstrapping procedure on a different measure, end of protraction to the end of B6/B9 activity in the suspended buccal mass, which has an AUC (0.632) that corresponds roughly to the desired effect size of a change in AUC of ±0.1 relative to the AUC for normalized duration of RN activity in the isolated ganglia (0.731); since the sampling distributions of AUCs are nearly independent of the underlying data distributions [S17], this bootstrapping procedure provided us with an approximate sampling distribution for the alternative hypothesis without making assumptions about the data distributions. The power analysis indicates that this test could detect changes in AUC of ±0.1 with power = 0.88.

Similarly, a difference in individuality in normalized duration of RN activity between the *in vivo* preparation (Figure 2A) and the SBM preparation (Figure S2C) was tested for significance by bootstrapping (this time, *in vivo* swallows were resampled). A two-tailed test was then performed to determine if the SBM AUC is significantly different from the *in vivo* AUC.

Again, we constructed an approximate sampling distribution for the alternative hypothesis by using the same bootstrapping procedure on a different measure, start of protraction to the end of closing in the suspended buccal mass, which has an AUC (0.708) that corresponds roughly to the desired effect size of a change in AUC of ±0.1 relative to the AUC for normalized duration of RN activity *in vivo* (0.610). The power analysis indicates that this test could detect changes in AUC of ±0.1 with power = 0.68.

Other power analyses

Power of Wilcoxon signed-rank two-tailed tests for detecting differences in within-animal variability and across-animal variability of ±5% for all 45 motor measures was determined to be 0.68.

Power of the test for correlation between changes in within- and across-animal variability presented in Figure 3A, and of tests for correlation between differences in

individuality and behavioral impact presented in Figures 3B and S3B and in the text for $|\varrho| > 0.35$ was determined to be 0.66.

Supplemental References

S1. Kupfermann I.(1974) Feeding behavior in *Aplysia*: a simple system for the study of motivation. Behav. Biol. *10*, 1–26.

S2. Cullins, M. J. and Chiel, H. J. (2010) Electrode fabrication and implantation in *Aplysia californica* for multi-channel neural and muscular recordings in intact, freely behaving animals. J. Vis. Exp. *40*, 1791, doi:10.3791/1791.

S3. Morton, D. W. and Chiel, H. J. (1993a) *In vivo* buccal nerve activity that distinguishes ingestion from rejection can be used to predict behavioral transitions in *Aplysia*. J. Comp. Physiol. A. *172*, 17-32.

S4. McManus, J. M., Lu, H. and Chiel, H. J. (2012) An *in vitro* preparation for eliciting and recording feeding motor programs with physiological movements in *Aplysia californica*. J. Vis. Exp. *70*, e4320, doi:10.3791/4320.

S5. Susswein, A. J., Rosen, S. C., Gapon, S. and Kupfermann, I (1996) Characterization of buccal motor programs elicited by a cholinergic agonist applied to the cerebral ganglion of *Aplysia californica*. J. Comp. Physiol. A. *179*, 509-24.

S6. Hurwitz, I, Neustadter, D., Morton, D. W., Chiel, H. J., and Susswein, A.J. (1996) Activity patterns of the B31/B32 pattern initiators innervating the I2 muscle of the buccal mass during normal feeding movements in *Aplysia californica*, J. Neurophysiol. *75*, 1309-1326.

S7. Morton, D. W. and Chiel, H. J. (1993b) The timing of activity in motor neurons that produce radula movements distinguishes ingestion-like and rejection-like motor patterns in a reduced preparation of *Aplysia*, J. Comp. Physiol. A. *173*, 519 - 536.

S8. Warman, E. N. and Chiel, H.J. (1995) A new technique for chronic single extracellular recording in freely behaving animals using pipette electrodes, J. Neurosci. Methods *57*, 161-169.

S9. Lu, H., McManus, J. M. and Chiel, H. J. (2013) Extracellularly identifying motor neurons for a muscle motor pool in *Aplysia californica*. J. Vis. Exp. *73*, e50189, doi:10.3791/50189.

S10. Church, P. J. and Lloyd, P. E. (1994) Activity of multiple identified motor neurons recorded intracellularly during evoked feeding-like motor programs in *Aplysia*. J. Neurophysiol. *72*, 1794-1809.

S11. Ye, H., Morton, D. W. and Chiel, H. J. (2006) Neuromechanics of coordination during swallowing in *Aplysia californica*. J. Neurosci. *26*, 1470-1485.

S12. Lu, H., McManus, J.M., Cullins, M. J. and Chiel, H. J. (2015) Preparing the periphery for a subsequent behavior: Motor neuronal activity during biting generates little force but prepares a retractor muscle to generate larger forces during swallowing in *Aplysia*. J. Neurosci. *35*, 5051 – 5066.

S13. Cullins, M. J., Shaw, K. M., Gill, J. P., and Chiel, H. J. (2015) Motor neuronal activity varies least among individuals when it matters most for behavior. J. Neurophysiol. *113*, 981 - 1000.

S14. Fawcett, T. (2006) An introduction to ROC analysis. Patt. Recog. Lett. *27*, 861 – 874.

S15. Krzanowski, W. J. and Hand, D. J. (2009) ROC Curves for Continuous Data (Boca Raton, FL: Chapman & Hall/CRC).

S16. Hand, D. J. and Till, R. J. (2001) A simple generalization of the area under the ROC curve for multiple class classification problems. Machine Learn. *45*, 171 – 186.

S17. Hanley, J. A. and McNeil, B. J. (1982) The meaning and use of the area under a receiver operating characteristic (ROC) curve. Radiology *143*, 29 – 36.